

Nanoscale

Accepted Manuscript



This is an *Accepted Manuscript*, which has been through the Royal Society of Chemistry peer review process and has been accepted for publication.

Accepted Manuscripts are published online shortly after acceptance, before technical editing, formatting and proof reading. Using this free service, authors can make their results available to the community, in citable form, before we publish the edited article. We will replace this *Accepted Manuscript* with the edited and formatted *Advance Article* as soon as it is available.

You can find more information about *Accepted Manuscripts* in the [Information for Authors](#).

Please note that technical editing may introduce minor changes to the text and/or graphics, which may alter content. The journal's standard [Terms & Conditions](#) and the [Ethical guidelines](#) still apply. In no event shall the Royal Society of Chemistry be held responsible for any errors or omissions in this *Accepted Manuscript* or any consequences arising from the use of any information it contains.

ARTICLE

Graphene-like BN/Gelatin nanobiocomposites for gas barrier applications

J. Biscarat,^a M. Bechelany,^a C. Pochat-Bohatier^a and P. Miele^a

Cite this: DOI: 10.1039/x0xx00000x

Received 00th January 2012,
Accepted 00th January 2012

DOI: 10.1039/x0xx00000x

www.rsc.org/

We report a simple, effective and green way for the fabrication of gelatin–graphene-like BN nanocomposites for gas barrier applications. The reinforcement effect of graphene-like BN on the gelatin properties is discussed. The obtained graphene-like BN nanocomposites show good dispersion in the gelatin matrix and remarkable capability to improve the crystallinity and the barrier properties of gelatin. The barrier properties of gelatin/BN nanocomposites have been enhanced by a factor of 500 at 2 bar comparing to a gelatin film without graphene-like BN. The greatly improved performance and the high stability of these nanocomposites induce exciting materials for their implantation in gas barrier applications.

A Introduction

Packaging materials production has a real impact on natural resources. The depletion of oil resources makes necessary to find new generations of bio-sourced polymers. However, it is not reasonable to consider large-scale use of materials derived from agricultural resources with high nutritional potential as soybeans or corn (e. g. polylactic acid). Gelatin is an attractive alternative because it is an industrial byproduct of hides and carcasses, cheap and abundant. It is a protein obtained by partial hydrolysis of collagen, a fibrous insoluble protein, which is widely found in nature as the major constituent of skin, bone and connective tissue.¹ It allows the preparation of biodegradable and biocompatible materials by methods developed without organic solvent. The gelatin films have low permeability to gas due to the semi-crystalline nature of the proteins.² Gelatin can be used as polymer constituent materials for the preparation of super barrier. Preliminary work has shown that the gelatin can be cross-linked to form water-insoluble films and resistant to water vapor.^{3–5} The field of drug packaging has many constraints (*i.e.* safety, neutrality, protection, cleanliness, and sterility). One of the current research topics in this field is the development of materials with very high barrier properties with the aim to approach the barriers of aluminum properties while maintaining transparency. Therefore, one of the methods to improve the barrier properties of Gelatin is the development of nanocomposites based on clay, graphene or graphene like nanostructures.^{6–11} This approach show high potentiality in designing green and eco-friendly nanobiocomposites with high improvement of thermal, mechanical and barrier properties.¹² Among the most used fillers, two-dimensional (2D) boron nitride crystals have attracted recently a great interest due to their structural similarities to graphene. The white graphene (monolayer of BN) is an individual h-BN basal plane in which C atoms have been fully substituted by alternating B and N atoms.¹³ Besides the conventional applications of boron nitride, novel properties can arise from the boron nitride nanosheets

(BNNS) due to the high surface area and the edge structures.¹⁴ BN monolayer demonstrated outstanding properties such as a high temperature stability, enhanced oxidation resistance (900°C under air), a large band gap (> 5 eV), low dielectric constant, high hardness (15–24 kg mm⁻²), high corrosion resistance, and large thermal conductivity (~6600 W m K⁻¹).¹⁵ These properties make BNNS a very appealing in wide range of applications such as nanoelectronic, optoelectronic and nanocomposites. Further applications in hydrogen storage, catalysis, sensing and robust coating have been as well explored.¹⁶ In addition BNNS have attractive attention for high performance polymeric composites. BNNS are stronger and more thermally conductive than graphene, have better oxidation resistance and thermal stability and do not absorb in the visible region.¹⁷

The fabrication of BNNS has been achieved by 2 approaches: the bottom up and the top down. The bottom-up approach usually involves the synthesis of BNNS from boron and nitrogen precursors using CVD methods for instance^{18, 19} and yields BNNS of large lateral sizes and low crystallinity. Alternatively, the top down techniques that mainly refer to the exfoliation of hexagonal Boron Nitride such as mechanical cleavage,²⁰ sonication-assisted direct solvent exfoliation,²¹ chemical functionalization,²² and the boron nitride nanotubes unzipping²³ provide highly crystalline BNNS with limited lateral sizes and a small percentage of BN single layers. Recently, Ge *et al.*²⁴ reported a gelatin-assisted technique for the fabrication of water-dispersible graphene and its inorganic analogues. The graphene has been used to prepare gelatin–graphene composites with enhanced mechanical properties.

In the present paper, a simple and effective way for the fabrication of gelatin–graphene-like BN nanobiocomposites for gas barrier applications is reported. We investigate the reinforcement effect of graphene-like BN on the gelatin properties. The obtained graphene-like BN nanobiocomposites show good dispersion in the gelatin matrix and remarkable capability to improve the crystallinity and the barrier properties of Gelatin. For our knowledge, this is the first report on the

barrier properties of graphene-like BN /Gelatin nanobiocomposites.

B Results and discussion

In order to study the influence of graphene-like BN incorporation on the gelatin film properties, three different samples have been elaborated and fully characterized: (i) a graphene-like BN /gelatin nanocomposites film (Ge-BN) prepared by sonification for 1 hour followed by centrifugation at 1500 rpm for 30 min and finally a casting at 500 μm thickness; (ii) a gelatin film (Ge-S) having undergone the same process (including ultrasonication) without BN; and (iii) a Gelatin (Ge) film elaborated without the sonification and the centrifugation steps to uncouple the effects of graphene-like BN and those of the elaboration process. All the films were easy to handle and flexible. Gelatin films (Ge and Ge-S) were transparent while Ge-BN films were translucent.

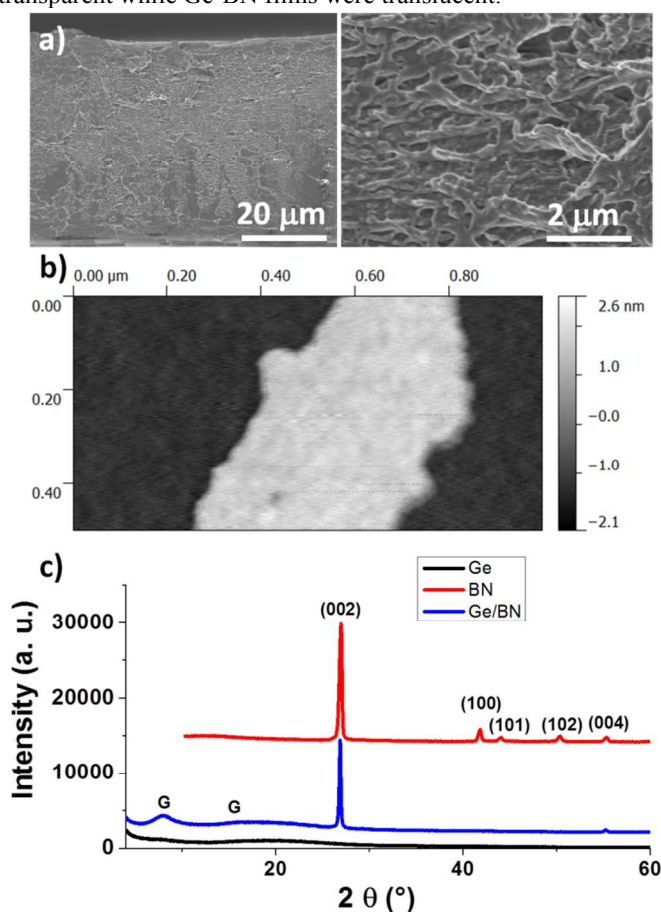


Figure 1. a) SEM cross section images at different magnifications of Ge-BN nanobiocomposites (EDX element mapping in supporting information: Figure S2), b) AFM image of Graphene-like BN and c) XRD diffraction of BN powders, graphene-like BN incorporated in Gelatin (Ge-BN) and a Gelatin standard film (Ge)

SEM (Figure 1a) was employed to evaluate the morphological characteristics of Ge-BN film nanobiocomposites. As can be seen from Figure 1a, the Graphene-like BN were randomly dispersed in the matrix, showing typical characteristics of good compatibility between the Graphene-like BN and the Gelatin

matrix. In addition, the SEM EDX cross section mapping of the GE-BN nanobiocomposites (Supporting Information: Figure S2) demonstrated that Graphene-like BN was homogeneously distributed on the Gelatin film. Atomic force microscopy (AFM) image (Figure 1b) indicated that the thickness of Graphene-like BN was around 1.5 nm with a lateral size of approximately $0.5 \times 1.0 \mu\text{m}$ giving evidence to a very efficient exfoliation of graphene-like BN in Gelatin (Supporting Information: Figure S3).

Figure 1c shows the XRD diffraction of BN powders, graphene-like BN incorporated in Gelatin and a Gelatin standard film. The XRD graphene-like BN incorporated in gelatin shows only 2 peaks at $2\theta = 26.801^\circ$ and 55.121° corresponding to (002) and (004) plane respectively of hexagonal boron nitride (BN). The peak at $2\theta = 41.691^\circ$, 43.911° and 50° corresponding to the (100), (101) and (102) planes of the h-BN, respectively were not observed. This confirms a very efficient exfoliation of graphene-like BN and dispersion in Gelatin. The graphene-like BN are well aligned along the gelatin film which induces the disappearing of the (100), (101) and (102) plane. The apparent crystallinity of gelatin was determined as well by XRD (Table 1).

Table 1. Crystallinity level of Ge, Ge-S and Ge-BN nanobiocomposites

	Crystallinity level (%)
Ge	30 ± 2
Ge-BN	34 ± 2
Ge-S	29 ± 2

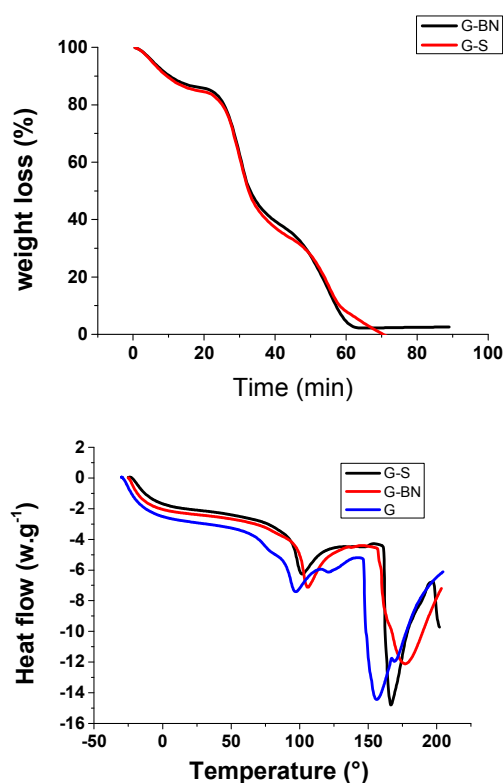


Figure 2. a) TGA of Ge-S and Ge-BN nanobiocomposites; b) DSC curves of Ge, Ge-S and Ge-BN nanobiocomposites

Gelatin diffractogram shows generally two peaks: one about 7° and one between 17 to 22° representing respectively the triple-helical crystalline structure and the amorphous part of gelatin.²⁵⁻²⁷ The crystallinity was determined considering the ratio between the area under the crystalline peak and the area under the amorphous halo following the method used by Charmette *et al.*²⁸ **Table 1** shows crystallinity level of Ge, Ge-S and Ge-BN nanobiocomposites. The results show that ultrasonification does not affect the crystallinity of Gelatin. An increase of the crystallinity is observed for Ge-BN samples. This improvement of crystallinity could be related to the electrostatic interaction or hydrogen bond between charged groups of gelatin chains and the graphene-like BN that induces nucleus sites for the crystallization of gelatin. Indeed, the crystallinity of gelatin is directly related to its triple helical structure which formation is believed to follow a nucleation and growth mechanism.²⁹

To study the effect of graphene-like BN addition on the thermal property of gelatin, thermogravimetric analysis (TGA) was performed under an oxygen flow of 60 mL/min (**Figure 2a**). Samples were heated until 600°C at 10°C/min and then equilibrated at 600°C for 30 min to insure the total degradation of the gelatin. The films tested were at the equilibrium meaning that after drying they were stored at 20°C in a box (ca. 25 ± 5 % RH). TGA analysis showed a 14% of weight loss for both samples (Ge-S and Ge) was observed at around 100°C due the water evaporation meaning that even after drying the Ge and Ge-S films still contained 14% of residual water. These 14% correspond to the high energy structural bond water involved in the formation and stabilization of the triple helical gelatin structure.²⁵ As expected no difference was observed between the Ge and Ge-S samples; the film's elaboration process did not had any impact on the final composition of the film.

From TGA analysis, it was observed that gelatin (Ge-S and Ge) will decompose completely where a white residue of 2 % is observed for the Ge-BN nanobiocomposites. Due to his high thermal stability, BN does not show a weight loss in this range of temperature. Thus TGA permitted to establish the final composition of the films (**Table 2**).

Table 2. Composition of Gelatin (Ge), Ge-S and Ge-BN nanobiocomposites extracted from TGA data

	Gelatin (%)	Water (%)	BN (%)
Ge	86 ± 1	14 ± 1	-
Ge-BN	85 ± 1	12.9 ± 0.9	2.3 ± 0.1
Ge-S	86 ± 1	14 ± 1	-

Table 3. Tg, degradation and denaturation temperature and Renaturation level extracted from DSC data

	Tg (°C)	Degradation Temperature (°C)	denaturation Temperature (°C)	Renaturation level (%)
Ge	74 ± 1 ^a	159 ± 3 ^a	96 ± 1 ^a	60 ± 6 ^a
Ge-BN	85 ± 1 ^b	176 ± 2 ^b	107 ± 1 ^b	66 ± 8 ^a
Ge-S	86 ± 1 ^b	164 ± 4 ^d	102 ± 2 ^b	50 ± 3 ^b

Lower case letters indicate the statistical significance within a column ($p \leq 0.05$)

Figure 2b shows the DSC curves of gelatin Ge, Ge-S and Ge-BN nanobiocomposites. Films were cooled from 25°C to -40°C and then heated up to 230°C with a 100°C/min heating rate. This high speed permitted a better peak resolution between the denaturation and the degradation endotherms and to determine glass transition temperature. The denaturation endotherm is directly related to the denaturation of the collagen like triple helix. By doing the ratio between the gelatin membrane denaturation enthalpy and the value of the denaturation enthalpy of pure porcine skin collagen, $\Delta H_{denat\ coll} = 47.8 \text{ J/g}$ ³⁰, the renaturation level can be directly calculated²⁹. The used gelatin (Ge) has a Tg peak at 74 °C and a denaturation temperature of 96°C. The ultrasonification (Ge-S) induced an increase of the Tg which is not affected by the graphene-like BN addition (Ge-BN). This result could be explained by the fragmentation of gelatin in ultrasonic bath. However an increase of the denaturation temperature is observed for Ge-BN samples (107 °C) with the increase of the renaturation level (66 %) that could be explained as follows: gelatin chains that intercalate into the graphene-like BN are restricted by the nanosheets, and the movement of segments is restrained.³¹ In addition there exists electrostatic electric interaction or hydrogen bond between charged groups of gelatin chains and the graphene-like BN that act as physical crosslinking and reduced the activity of the gelatin. The DSC curve shows as well an increase of the gelatin degradation temperature (**Table 3**).³²

The mechanical properties (**Figure 3**) show that the ultrasonification decreases the Young's Modulus and the tensile strain break (MPa) of gelatin (Ge-S). This observation is related to the fragmentation of gelatin in ultrasonic bath as observed by DSC measurement. However the addition of graphene-like BN increased again the Young's Modulus and the tensile strain at break (MPa) of gelatin (Ge-BN) indicating a reinforcement of the biopolymer matrix by the graphene-like BN load. These results may suggest that the graphene-like BN were well dispersed in the gelatin matrix, and agree with Cyras *et al.*³³ and Rao *et al.*³⁴ who also observed good improvement in mechanical properties of gelatin-based nanocomposites by loading nanocharges inside the Gelatin.

The gelatin based nanobiocomposites have been studied for oxygen barrier applications. The oxygen permeability of Gelatin and Gelatin loaded with graphene-like BN are depicted in **Table 5**. Sonicated Gelatin could not be tested since the films broke during the experiment. Indeed their lower tensile stress at break value (**Table 4**) did not allowed the samples to undergo the vacuum treatment. Gelatin is a semipermeable or permeable material as the function of the pressure. The dispersion of graphene-like BN in the gelatin matrix will provide huddles to oxygen entrance. Table 5 shows that the barrier properties of gelatin/BN nanobiocomposites have been enhanced by a factor of 20 at 1.5 bar comparing to a gelatin film without graphene-like BN. This enhancement has been increased to 500 at 2 bar. The substantial reduction in oxygen permeability may be due to the good dispersion of graphene-like BN in gelatin matrix as demonstrated by XRD and EDX data, to the alignment of the graphene-like BN along the film as demonstrated as well by the XRD data and to the good interaction between the Gelatin and the graphene-like BN as shown by the thermal analysis and the mechanical properties.

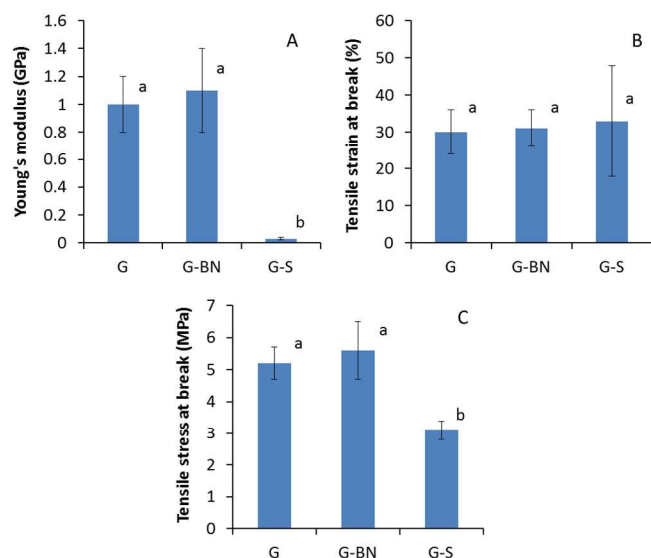


Figure 3. Young's modulus (A), tensile strain at break (B), and tensile stress at break (C) of Ge, Ge-S and Ge-BN nanocomposites. Lower case letters indicate the statistical significance ($p \leq 0.05$)

Table 4. Young's modulus and tensile strain at break (b, c) of Ge, Ge-S and Ge-BN nanobiocomposites

	Young's Modulus (GPa)	T strain (%)	T stress (Mpa)
Ge	1 ± 0.2^a	30 ± 6^a	5.2 ± 0.5^a
Ge-BN	1.1 ± 0.3^a	31 ± 5^a	5.6 ± 0.9^a
Ge-S	0.03 ± 0.01^b	33 ± 15^a	3.1 ± 0.3^b

Table 5. Oxygen barrier properties of Ge and Ge-BN nanocomposites as the function of the temperature.

	At 1.5 Bar (Barrer)	At 2 Bar (Barrer)
Ge	1.4 ± 0.2^a	25 ± 3^a
Ge-BN	0.07 ± 0.01^b	0.05 ± 0.01^b

C Experimental

1 Elaboration of Gelatin/ graphene-like BN nanocomposites.

BN powder (95294, 4-7 μm) was purchased from H.C STARCK and gelatin was bought from Sigma Aldrich. Gelatin (lot#0001409228) has a Bloom of 188g. A gelatin solution (20 % wt) was prepared by dissolving gelatin powder in distilled water under magnetic stirring at 60° C for one hour. BN powder with ratio 1/20 (BN/Gelatin mass ratio) was added to the aqueous solution and treated with an ultrasonic probe system (SONOPULS HD 3100) for 1 hour (pulse on/off for 1 second) with an amplitude of 60% to prepare a Gelatin/ graphene-like BN stable dispersion. The mixture was then centrifuged at 1500 rpm for 30 min to isolate the stable graphene-like BN dispersion from the unexfoliated BN powder.

Finally, the solution will be stored at 50°C for 12 hours for degassing. Films were prepared by dry-casting of the gelatin solution at 30°C on flat Teflon coated sheets with a K Control

Coater 101 (Erichsen Instruments). The solution was cast at 500 μm with an Erichsen Mod. 411 0956 casting knife. Gelatin films were allowed to dry at 20°C under (45 \pm 5)% Relative Humidity (RH) during 1 day. After getting off from their support, all the self-supported films were stored at 20°C in a desiccant box (ca. 25 \pm 5 %RH) before subsequent analysis.

2 Characterization.

Structural characterizations have been performed using a scanning electron microscopy (SEM, Hitachi S-4800). EDX measurement was carried out using a Zeiss EVO ED15 microscope coupled with a Oxford X-MaxN EDX detector. AFM measurements were realized using AFM NANOMAN 5 from Veeco instrument controlled with a Nanoscope V software on Graphene-like BN deposited on Silicon wafer. In order to eliminate the Gelatin, the sample has been annealed at 600°C under air.

The apparent crystallinity was determined by X-ray diffraction (PanAnalytical X'pert-Pro diffractometer). To eliminate the uncertainty due to the gelatin water content, the experiments were conducted in a sealed chamber (Anton Paar HT1200) after 15 hours under vacuum, at room temperature. The crystallinity was determined considering the ratio between the area under the crystalline peak and the area under the amorphous halo following the method used by Charmette *et al.*²⁸. Gelatin diffractogram shows two peaks: one about 7° and one between 17 to 22° representing respectively the triple-helical crystalline structure and the amorphous part of gelatin.²⁵⁻²⁷

Thermal properties were determined on dried films equilibrated at 25 \pm 5 % RH. Their residual humidity and the BN content was measured by thermogravimetric analysis (TGA) performed on a TA Instruments TGA G500 under an oxygen flow of 60 mL/min in the oven and a nitrogen flow of 40 mL/min for the scale. Samples around 10 mg were heated until 600°C at 10°C/min and then equilibrated at 600°C for 30 min to insure the total degradation of the gelatin.

The films were then analyzed using a differential scanning calorimeter DSC 2920 equipped with cooling accessory RCS90 (TA Instruments). The samples (\approx 6 mg) were sealed in aluminum TA pan. The instrument was calibrated with pure indium ($T_m = 156.6^\circ\text{C}$ and $\Delta H_m = 28.3 \text{ kJ/kg}$) and used an empty pan as reference. Films were cooled from 25°C to -40°C and then heated up to 230°C with a 100°C/min heating rate. This high speed permitted a better peak resolution between the denaturation and the degradation endotherms and to determine glass transition temperature (Figure S1). The denaturation endotherm is directly related to the denaturation of the collagen like triple helix. By doing the ratio between the gelatin membrane denaturation enthalpy and the value of the denaturation enthalpy of pure porcine skin collagen, $\Delta H_{\text{denat coll}} = 47.8 \text{ J/g}$ ³⁰, the renaturation level can be directly calculated²⁹.

The mechanical properties of the films were evaluated by extensional rheology. These tests were performed using a rheometer MCR 301 (Anton Paar) using the Universal Extensional Fixture UXF12. The temperature was controlled at 25°C thanks to CTD180 Peltier system. The samples tested were 4x1 cm² rectangles cut in different parts of the films (at least 3 per formulation). The protocol of these measurements followed 3 steps (Table S1).

Film thickness was determined using a thickness gauge (Mitutoyo). Measurements were performed on 10 points and gave a mean value.

3 Gas permeability.

The permeability of nanobiocomposites films has been measured for single gas series (O₂) by using the constant-volume and variable-pressure technique in a permeability apparatus at 25 °C, described in the standard ASTM D 1434-82 (procedure V). The apparatus consists essentially of a two compartments stainless steel permeation cell separated by the tested membrane equipped with silicon o-rings. The permeability was obtained measuring the pressure increase in the downstream compartment (with a constant volume of $5.25 \times 10^{-5} \text{ m}^3$) and using different MKS Baratron pressure transducers (range from 0.0 to $1 \times 10^5 \text{ Pa}$). The films and downstream cell walls were outgassed in situ during 24 h at high vacuum using a turbomolecular pump (Leybold, Turbovac 50, 50 l.s^{-1}). The permeability experiments were performed at 25 °C and increasing transmembrane pressure (ΔP) from 1 to 2 bars in order to detect any viscous flow contribution characteristic for the presence of macrodefects in the film. The pressure increase in the downstream compartment was monitored during 4 hours. For each condition change, the whole setup was allowed to stabilize during at least 12 hours. The magnitude of purity of gas used (O₂) was of 99.95%, they were used without any further purification. A complete description of the apparatus and methodology used was already published³⁵. Curves obtained presented only a pseudo steady state region. For calculations of the permeability, the mathematical treatment for thin films based on Fick's second law and reported by Crank was used.³⁶ The estimated error on the analysis was measured at $\pm 10 \%$. Statistical tests were performed using the computer program R. Differences between pairs of means were compared using a Kruskal-Wallis one-way analysis of variance test to avoid false positive response in case of non-normal distribution. The level of significance was set at $p \leq 0.05$.

Conclusions

In conclusion Gelatin/BN nanobiocomposites were synthesized by low cost green technique where water was used as the solvent. The dispersion of graphene-like BN in gelatin matrix was studied by SEM, EDX, AFM, XRD and thermal analysis (TGA and DSC). The results show an efficient exfoliation of graphene-like BN that aligned along the gelatin film. An improvement of the gelatin crystallinity is also observed. The Young's modulus and tensile strain at break measurements show that the addition of Graphene-like BN permitted to recover the mechanical properties loss during the sonication step. The barrier properties of gelatin/BN nanocomposites have been enhanced by a factor of 500 at 2 bar comparing to a gelatin film without graphene-like BN and O₂ permeability fall to 0.05 Barrer. The greatly improved performance and the high stability of these nanobiocomposites made with a bio-sourced polymer induce exciting materials for their implantation in gas barrier applications.

Notes and references

^a Institut Européen des Membranes, UMR 5635 CNRS Université Montpellier 2, Place Eugène Bataillon, F-34095 Montpellier cedex 5, France
mikhail.bechelany@univ-montp2.fr, Phone: +33467149167, Fax: +33467149119.

Electronic Supplementary Information (ESI) available: See DOI: 10.1039/b000000x/

1. M. C. Gomez-Guillen, B. Gimenez, M. E. Lopez-Caballero and M. P. Montero, *Food Hydrocolloids*, 2011, **25**, 1813-1827.
2. J. Biscarat, C. Charmette, J. Sanchez and C. Pochat-Bohatier, *Canadian Journal of Chemical Engineering*, 2014, DOI: 10.1002/cjce.22077.
3. A. Bigi, G. Cojazzi, S. Panzavolta, K. Rubini and N. Roveri, *Biomaterials*, 2001, **22**, 763-768.
4. M. Catalina, G. E. Attenburrow, J. Cot, A. D. Covington and A. P. M. Antunes, *Journal of Applied Polymer Science*, 2011, **119**, 2105-2111.
5. R. A. Carvalho, C. R. F. Grosso and P. J. A. Sobral, *Packaging Technology and Science*, 2008, **21**, 165-169.
6. J. T. Chen, Y. J. Fu, Q. F. An, S. C. Lo, Y. Z. Zhong, C. C. Hu, K. R. Lee and J. Y. Lai, *Carbon*, 2014, **75**, 443-451.
7. H. Kim, Y. Miura and C. W. Macosko, *Chem. Mat.*, 2010, **22**, 3441-3450.
8. G. Scherillo, M. Lavorgna, G. G. Buonocore, Y. H. H. Zhan, H. S. S. Xia, G. Mensitieri and L. Ambrosio, *ACS Appl. Mater. Interfaces*, 2014, **6**, 2229-2233.
9. J. T. Chen, Y. J. Fu, Q. F. An, S. C. Lo, S. H. Huang, W. S. Hung, C. C. Hu, K. R. Lee and J. Y. Lai, *Nanoscale*, 2013, **5**, 9081-9088.
10. Y. H. Yang, L. Bolling, M. A. Priolo and J. C. Grunlan, *Advanced Materials*, 2013, **25**, 503-508.
11. H. Y. Liu, T. Kuila, N. H. Kim, B. C. Ku and J. H. Lee, *J. Mater. Chem. A*, 2013, **1**, 3739-3746.
12. J. F. Martucci, A. Vazquez and R. A. Ruseckaite, *Journal of Thermal Analysis and Calorimetry*, 2007, **89**, 117-122.
13. A. Pakdel, C. Zhi, Y. Bando and D. Golberg, *Materials Today*, 2012, **15**, 256-265.
14. X. Wang, A. Pakdel, J. Zhang, Q. Weng, T. Zhai, C. Zhi, D. Golberg and Y. Bando, *Nanoscale Research Letters*, 2012, **7**.
15. Y. Yao, Z. Lin, Z. Li, X. Song, K.-S. Moon and C.-P. Wong, *Journal of Materials Chemistry*, 2012, **22**, 13494-13499.
16. K. R. Koswattage, I. Shimoyama, Y. Baba, T. Sekiguchi and K. Nakagawa, *Journal of Chemical Physics*, 2011, **135**.
17. Y. Lin and J. W. Connell, *Nanoscale*, 2012, **4**, 6908-6939.
18. M. Bechelany, A. Brioude, S. Bernard, P. Stadelmann, D. Cornu and P. Miele, *Crystengcomm*, 2011, **13**, 6526-6530.
19. R. Gao, L. Yin, C. Wang, Y. Qi, N. Lun, L. Zhang, Y.-X. Liu, L. Kang and X. Wang, *Journal of Physical Chemistry C*, 2009, **113**, 15160-15165.
20. K. S. Novoselov, D. Jiang, F. Schedin, T. J. Booth, V. V. Khotkevich, S. V. Morozov and A. K. Geim, *Proceedings of the National Academy of Sciences of the United States of America*, 2005, **102**, 10451-10453.
21. R. J. Smith, P. J. King, M. Lotya, C. Wirtz, U. Khan, S. De, A. O'Neill, G. S. Duesberg, J. C. Grunlan, G. Moriarty, J. Chen, J. Wang, A. I. Minett, V. Nicolosi and J. N. Coleman, *Advanced Materials*, 2011, **23**, 3944+.
22. W.-Q. Han, L. Wu, Y. Zhu, K. Watanabe and T. Taniguchi, *Applied Physics Letters*, 2008, **93**.
23. H. Zeng, C. Zhi, Z. Zhang, X. Wei, X. Wang, W. Guo, Y. Bando and D. Golberg, *Nano Letters*, 2010, **10**, 5049-5055.
24. Y. Ge, J. Wang, Z. Shi and J. Yin, *Journal of Materials Chemistry*, 2012, **22**, 17619-17624.
25. I. Yakimets, N. Wellner, A. C. Smith, R. H. Wilson, I. Farhat and J. Mitchell, *Polymer*, 2005, **46**, 12577-12585.
26. C. Andreuccetti, R. A. Carvalho, T. Galicia-Garcia, F. Martinez-Bustos and C. R. F. Grosso, *Journal of Food Engineering*, 2011, **103**, 129-136.
27. S. Rivero, M. A. Garcia and A. Pinotti, *Innovative Food Science & Emerging Technologies*, 2010, **11**, 369-375.
28. C. Charmette, J. Sanchez, P. Gramain and N. Masquelez, *J. Membr. Sci.*, 2009, **344**, 275-280.
29. D. Achet and X. W. He, *Polymer*, 1995, **36**, 787-791.
30. V. Samouillan, F. Delaunay, J. Dandurand, N. Merbahi, J.-P. Gardou, M. Yousfi, A. Gandaglia, M. Spina and C. Lacabanne, *Journal of functional biomaterials*, 2011, **2**, 230-248.

31. J. P. Zheng, P. Li, Y. L. Ma and K. D. Yao, *Journal of Applied Polymer Science*, 2002, **86**, 1189-1194.
32. S. K. Swain, S. Dash, C. Behera, S. K. Kisku and L. Behera, *Carbohydrate Polymers*, 2013, **95**, 728-732.
33. V. P. Cyras, L. B. Manfredi, M.-T. Ton-That and A. Vazquez, *Carbohydrate Polymers*, 2008, **73**, 55-63.
34. Y. Rao, *Polymer*, 2007, **48**, 5369-5375.
35. C. Joly, S. Goizet, J. C. Schrotter, J. Sanchez and M. Escoubes, *J. Membr. Sci.*, 1997, **130**, 63-74.
36. J. Crank, *The Mathematics of Diffusion*, Clarendon Press, Oxford, 1975.

Table of contents

We report a simple, effective and green way for the fabrication of gelatin–graphene-like BN nanocomposites for gas barrier applications.

